Progress In Electromagnetics Research, PIER 103, 201–216, 2010

DOA ESTIMATION WITH SUB-ARRAY DIVIDED TECHNIQUE AND INTERPORLATED ESPRIT ALGORITHM ON A CYLINDRICAL CONFORMAL ARRAY ANTENNA

P. Yang, F. Yang, and Z. P. Nie

School of Electronic Engineering
University of Electronic Science and Technology of China (UESTC)
Chengdu 610054, China

Abstract—A novel DOA finding method for conformal array applications is proposed. By using sub-array divided and interpolation technique, ESPRIT-based algorithms can be used on conformal arrays for 1-D and 2-D DOA estimation. In this paper, the circular array mounted on a metallic cylindrical platform is divided to several sub-arrays, and each sub-array is transformed to virtual uniform linear array or virtual uniform planar array through interpolation technique. 1-D and 2-D direction of arrivals can be estimated accurately and quickly by using LS-ESPRIT and 2-D DFT-ESPRIT algorithms, respectively. This method can be applied not only to cylindrical conformal array but also to any other arbitrary curved conformal arrays. Validity of this method is proved by simulation results.

1. INTRODUCTION

Conformal antenna array, i.e., array antennas with antenna elements arranged conformal on a curved surface, is of interest for future communication and defense applications [1, 2]. In contrast to ordinary arrays, when cylindrical conformal array is used for wide range (more than 90 degrees) DOA (direction of arrival) estimation, several problems must be considered. Firstly, conformal array has the "shadow effect" because of the metallic cylinder, which means for an incident wave from a special angle, and not all of the antenna elements can receive this signal. Secondly, the radiation pattern of antenna element cannot be regarded as omni-directional since the platform behaves as

Corresponding author: P. Yang (yangpeng@eee.hku.hk).

a metallic ground. Therefore, for a conformal array, the elements' radiation patterns are always directional. Thirdly, the mutual coupling between elements becomes more complicated and cannot be ignored. These characters make it difficult to use normal DOA estimation algorithms on conformal arrays for DOA finding.

Most high resolution DOA estimation algorithms, such as MUSIC-based and ESPRIT-based algorithms, when used on uniform liner array with omni-directional antenna elements, they always have high performance [3–5]. But usually, these algorithms cannot be used for conformal array directly. For example, MUSIC algorithm can estimate the signal's DOA accurately for any array geometry, but if the array's steering vector is incomplete (e.g., when a circular array is mounted on a metallic cylindrical surface, for a signal with special DOA, some antenna elements cannot receive this signal. In this situation, the steering vector of this circular array is incomplete), the performance of MUSIC algorithm deteriorates quickly. Sub-array divided MUSIC algorithm can solve this problem efficiently [6]. However, the complexity of the spectral searching in the conventional MUSIC algorithm may still be too high. Therefore, it is not fit for real-time applications. ESPRIT algorithm is a search-free DOA estimation algorithm. It exhibits lower computation and storage requirements than MUSIC algorithm by using a displacement invariant array. Unfortunately, in most cases, ESPRIT algorithm can only be applied to uniform linear array because it requires arrays that consist of two identical and identically oriented sub-arrays. Phase mode based ESPRIT algorithm can be applied to uniform circular array but not to conformal array, because the periodic excitation condition will be destroyed due to the incomplete steering vector [7]. To apply these algorithms to arrays with arbitrary geometries, interpolation technique is a good choice [8–11]. Recently, some interpolation based methods have been proposed for DOA estimation [12, 13].

In this paper, sub-array divided and interpolated ESPRIT methods are combined together for 1-D and 2-D DOA estimation on conformal array. The DOAs can be estimated accurately in 360° range by dividing a cylindrical conformal array into 8 sub-arrays. Simulation results exhibit the efficiency and accuracy of this method. This paper is organized as follows. In Section 2, interpolated ESPRIT algorithm based on sub-array divided technique is proposed in detail, and both 1-D and 2-D problems are discussed. In Section 3, a few of numerical simulation examples are given and compared with MUSIC algorithm. Finally, the new method is concluded in Section 4.

2. INTERPOLATED ESPRIT BASED ON SUB-ARRAY DIVIDED TECHNIQUE

2.1. Cylindrical Conformal Array

Figure 1 represents a cylindrical conformal array, and M microstrip antennas are uniformly distributed over the circumference of a radius r in the x-y plane. Fig. 2 shows the radiation pattern of E_θ of single element. At time t, assuming that there are $P\,(P < M)$ narrowband signals come from far field of the array with azimuth $\phi_i\,(i = 1, 2, \ldots, p)$ and impinge on the antenna array, the $M \times 1$ output vector of the array is given by

$$\mathbf{X}(t) = \mathbf{F}(\phi) \cdot \mathbf{A}(\phi)\mathbf{S}(t) + \mathbf{n}(t) \tag{1}$$

where $\mathbf{S}(t)$ is a $P \times 1$ vector whose ith element corresponds to the ith signal. $\mathbf{A}$ is a $M \times P$ steering matrix, whose columns are the steering vectors of the P signals on the array. The $M \times 1$ vector $\mathbf{n}(t)$ represents additive noise. $\mathbf{F}$ is a $M \times P$ radiation pattern matrix, which denotes mth $(m = 1, 2, \ldots, M)$ antenna's response to pth $(p = 1, 2, \ldots, P)$ signal

$$\mathbf{F} = [\mathbf{f}(\phi_1), \mathbf{f}(\phi_2), \ldots, \mathbf{f}(\phi_p)] \tag{2}$$

$$\mathbf{f}(\phi_p) = [f(\phi_p - \beta_1), f(\phi_p - \beta_2), \ldots, f(\phi_p - \beta_M)]^T \tag{3}$$

where $f(\phi_p - \beta_m)$ is mth element's response at ϕ_p, and $(\cdot)^T$ denotes the transpose and $\beta_m = 2\pi(m-1)/M$.

Unlike ordinary circular array, conformal array has the "shadow effect" due to the metallic cylinder, which means for a signal comes from angle ϕ, and not all elements can receive this signal. For example,

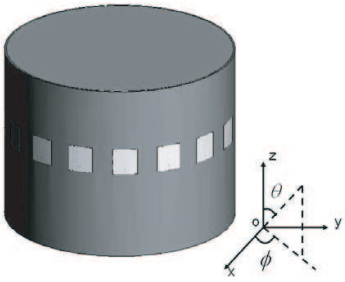

Figure 1. 16-element conformal array.

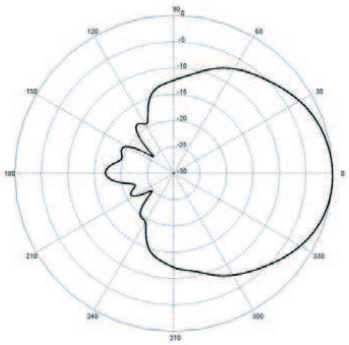

Figure 2. Radiation pattern of E_θ for single element.

if a signal with DOA of $\pi/2$ impinges on this array, from Fig. 3, it is clear to see that only number 1–9 elements can receive this signal, and the signal's steering vector can be expressed as

$$\mathbf{a}\left(\frac{\pi}{2}\right)=\left[1,\, e^{jkr\cos\left(\frac{\pi}{2}-\frac{\pi}{8}\right)},\, e^{jkr\cos\left(\frac{\pi}{2}-\frac{\pi}{4}\right)},\, \ldots,\, e^{jkr\cos\left(\frac{\pi}{2}-\pi\right)},\, 0,\, \ldots,\, 0\right]^T \tag{4}$$

where $k = 2\pi/\lambda$ is the wave number, and λ is the wavelength of the signal, $j = \sqrt{-1}$. It can be seen that the steering vector is incomplete for the conformal array because there are some zero elements in this vector. This incomplete steering vector will cause many problems in high performance DOA algorithms. For instance, it is well known in MUSIC algorithm that the noise subspace $\mathbf{U}_N$ is derived from the decomposition of the covariance matrix $\mathbf{R}_{xx}$. When MUSIC algorithm is applied to such a conformal array, $\mathbf{U}_N$ is incomplete because the incomplete steering vector $\mathbf{a}$ will cause an incomplete covariance matrix $\mathbf{R}_{xx}$. If we use a complete steering vector $\mathbf{a}_c$ to construct the MUSIC spectrum

$$P_{\text{MUSIC}} = \frac{1}{\mathbf{a}_c^H(\phi)\mathbf{U}_N\mathbf{U}_N^H\mathbf{a}_c(\phi)} \tag{5}$$

where symbol '**H**' means conjugate transpose. It is obvious that $\mathbf{a}_c^H\mathbf{U}_N \neq 0$ even in the case of noise absence. So the performance of MUSIC algorithm will be poor.

Another problem for conformal array is that each antenna element has a different response to a certain signal. In Fig. 3, if the signal comes from $\phi = \pi/2$, antenna 5 has the strongest response while antennas 1 and 9 can hardly receive this signal due to the directional radiation patterns. Traditional DOA estimation algorithms always assume that all elements can receive all signals, and each element has an omni-directional radiation pattern. These algorithms cannot be used on conformal array directly because these algorithms are sensitive to the environment, and the different element response will lead a big estimation error.

2.2. Sub-array Divided Technique

To eliminate the effects that result from incomplete steering vector, we can divide the whole array into 8 sub-arrays, and each sub-array spans a sector of $\pi/2$, i.e., in Fig. 3, element 1–5 compose sub-array 1, element 3–7 compose sub-array 2, etc. Through this way, for any signal, we can always find a sub-array, all whose elements can receive the signal, which means its steering vector is "complete". It is worth to note that each sector should be no larger than $\pi/2$, because for each sub-array, if its span sector is over $\pi/2$, there would exist a "blind spot"

that cannot receive the signal, which will lead to a incomplete steering vector. The searching space is also divided into 8 sub-sectors. It is well known that the antenna array has higher estimation performance when the DOA of the signal close to the normal direction of the array, that is to say, for sub-array 1 in Fig. 3, the corresponding searching sector is chosen from $\pi/16$ to $3\pi/16$. For sub-array 2, the searching sector is from $3\pi/16$ to $5\pi/16$, etc. Using this technique, a sub-array divided MUSIC algorithm can be derived and applied to any arbitrary conformal arrays.

2.3. Interpolated Array

The principle of interpolated array is dividing the field of view of the array into L sectors. The size of the sectors depends on the array geometry and on the desired interpolation accuracy. For example, if there is a signal, whose DOA is in the sector $\mathbf{\Phi} \in [\phi_1, \phi_2]$, where ϕ_1 and ϕ_2 are the left and right boundaries of this sector, let $\Delta\phi$ as the interpolation step, then $\mathbf{\Phi}$ can be represented as

$$\mathbf{\Phi} = [\phi_1, \phi_1+\Delta\phi, \phi_1+2\Delta\phi, \ldots, \phi_1+n\Delta\phi, \phi_2] \tag{6}$$

The interpolation number n is determined by the desired accuracy. In this sector, the real array manifold is

$$\mathbf{F} \cdot \mathbf{A} = [\mathbf{f}(\phi_1)\mathbf{a}(\phi_1), \mathbf{f}(\phi_1+\Delta\phi)\mathbf{a}(\phi_1+\Delta\phi), \ldots, \mathbf{f}(\phi_2)\mathbf{a}(\phi_2)] \tag{7}$$

We can construct an interpolated virtual array steering matrix $\bar{\mathbf{A}}$ in the same sector with omni-directional radiation pattern

$$\bar{\mathbf{A}} = [\bar{\mathbf{a}}(\phi_1), \bar{\mathbf{a}}(\phi_1 + \Delta\phi), \ldots, \bar{\mathbf{a}}(\phi_2)] \tag{8}$$

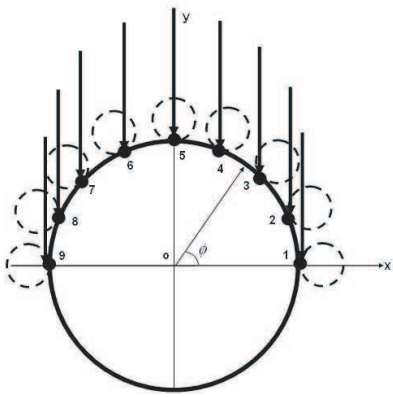

Figure 3. Signal impinges from $\phi = \pi/2$.

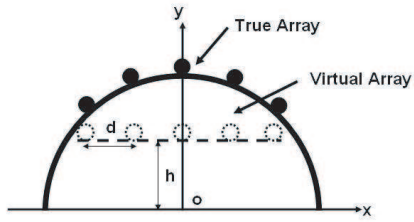

Figure 4. Real and virtual sub-array 2.

Then an interpolation matrix $\mathbf{B}$ is designed to satisfy in the least square sense, that is

$$\mathbf{B}^H[\mathbf{F} \cdot \mathbf{A}(\phi)] = \bar{\mathbf{A}}(\phi), \quad \phi \in \mathbf{\Phi} \tag{9}$$

The size of $\mathbf{B}$ is $M \times M$. Obviously, it is impossible to find an ideal $\mathbf{B}$ to satisfy Equation (9). The accuracy of the interpolation is examined by comparing the ratio of the Frobenius norms

$$\tau = \frac{|| \left(\bar{\mathbf{A}} - \mathbf{B}^H(\mathbf{F} \cdot \mathbf{A}\right) ||}{||\mathbf{F} \cdot \mathbf{A}||} \tag{10}$$

If τ is small enough, for example, 0.001, then accept $\mathbf{B}$. If this ratio is not sufficiently small, we can reduce $\Delta\phi$ or change the form of the interpolation array and recalculate it. It can be seen that the interpolation procedure is time consuming if the sector size and the number of interpolation angle n are very large. Fortunately, this procedure can be done off-line. The matrix $\mathbf{B}$ just needs to compute only once for any given array then stored in the system.

2.4. 1-D Interpolated ESPRIT

ESPRIT is an efficient algorithm for DOA estimation. It has lower computation than MUSIC based algorithms due to its search-free character. This advantage is achieved by using a displacement invariant array. However, ESPRIT algorithm usually can only be used on uniform linear array or uniform circular array. By using sub-array divided and interpolated techniques, the conformal array is transformed to 8 uniform linear arrays, and then ESPRIT algorithm can be used on each sub-array to estimate the DOA coming from corresponding observation sector. This method can be summarized by the following steps:

1) Divide the whole array into 8 sub-arrays using the method denoted in 2.2;
2) For each one-quarter circular sub-array, using the interpolated technique to find a series of matrix $\mathbf{B}_i$ ($i = 1, 2, \ldots, 8$) and transform it to virtual uniform linear array. Fig. 4 shows the real and virtual sub-array 2. Because the structure is symmetrical, for different sub-arrays, the transform matrix $\mathbf{B}_i$ is identical. In the procedure of finding $\mathbf{B}$, there are two key parameters which need to be optimized, the distance d between two elements of virtual uniform linear array and distance h from the original point to the virtual array.
3) Use formula (1) to get the receiving data vector $\mathbf{X}(t) = [x_1(t), \ldots, x_M(t)]^T$. Let $\mathbf{X}_i(t) = [x_{i1}(t), \ldots, x_{i5}(t)]^T$ denote the data vector of ith sub-array which is obtained from step 1.

4) Compute the interpolation receiving data for each virtual sub-array by using the interpolation matrix $\mathbf{B}$

$$\mathbf{Y}_i = \mathbf{B}\mathbf{X}_i \tag{11}$$

5) Estimate the DOA using LS-ESPRIT algorithm on each sub-array.

Step 1) and 2) above are a preprocess procedure. Once the virtual array is selected, the matrix $\mathbf{B}$ can be calculated off-line and stored in the system.

2.5. 2-D Interpolated ESPRIT

Figure 5 shows a 2-D cylindrical conformal array. For this 2-D array, we can transform it to virtual uniform planar array by using the interpolation method discussed above. This transformation is shown in Fig. 6. Unlike 1-D case, the normal ESPRIT algorithm cannot be used for a planar array directly, because the fundamental theorem of algebra does not hold in two dimensions, which may preclude to get a rooting type formulation. For uniform planar array, we can decompose the 2-D problem into two 1-D problems by using the 2-D DFT beam space ESPRIT algorithm [14]. Compare to 1-D ESPRIT, 2-D DFT interpolated ESPRIT needs two steps. The first step is to find the interpolation matrix $\mathbf{B}$ as 1-D case, and this matrix is used to transform the 2-D cylindrical conformal array to virtual uniform planar array. To find $\mathbf{B}$, 2-D interpolation is needed, and Equation (6) can be replaced by

$$[\mathbf{\Phi}, \mathbf{\Theta}] = [(\phi, \theta)_1, (\phi, \theta)_2, \ldots, (\phi, \theta)_K] \tag{12}$$

Figure 5. 5 by 5 cylindrical conformal array.

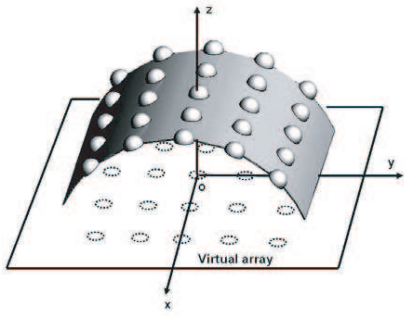

Figure 6. Real conformal array and virtual planar array.

where, $K = K_1 \times K_2$, K_1 is the interpolation number in ϕ direction and K_2 in θ direction. It is clear to see that 2-D problem needs much more interpolation points than 1-D problem.

The second step is to transform the receiving data from element space to beam space

$$\mathbf{D} = \mathbf{W}^H \mathbf{Y} \tag{13}$$

where $\mathbf{Y} = \mathbf{BX}$ is the interpolation receiving data, and $\mathbf{D}$ is the beam space receiving data. $\mathbf{W} = [\mathbf{w}_0, \mathbf{w}_1, \ldots, \mathbf{w}_{M-1}]$ and

$$\mathbf{w}_m^H = e^{j\left(\frac{M-1}{2}\right)m\frac{2\pi}{M}} \cdot \left[1, e^{-jm\frac{2\pi}{M}}, e^{-j2m\frac{2\pi}{M}}, \ldots, e^{-j(M-1)\frac{2\pi}{M}}\right] \tag{14}$$

After this processing, we can use 2-D DFT ESPRIT algorithm to estimate 2-D DOAs for this virtual uniform planar array. The procedure for 2-D problem is similar to what has been discussed in Section 2.4.

3. SIMULATION RESULTS

Simulations are conducted to evaluate the performance of the proposed method. The first example presented in this section uses the model shown in Fig. 1. 16 microstrip antennas are mounted on the surface of the metallic cylinder. The antenna elements are square patches, and the operating frequency is 3 GHz. There is a thin dielectric with permittivity of 4.3 and thickness of 2 mm between the cylinder and patch. The E-field of the antenna is along the z-axial. The cylinder's height is 3λ, and radius is 1.28λ. Here λ is the resonant wavelength. The E-plane (x-z) pattern of element 1 ($\phi = 0$) is calculated by using the method of moment (MOM), shown in Fig. 2. All the antenna elements have identical radiation pattern due to the symmetrical structure.

In order to get an ideal transformation matrix $\mathbf{B}$, three key points need to be mentioned. Firstly, the virtual array steering vector must be chosen properly. Here we choose the uniform linear array as the virtual array, and the parameters d and h shown in Fig. 4 need to be optimized. Fig. 7 shows the optimization result. It can be seen that when $d = 0.51\lambda$ and $h = 0.83\lambda$, the error is the smallest, about 8.2×10^{-4}. Secondly, the interpolation sector cannot be selected too large. As shown in Fig. 8, when the interpolation sector is over 60°, the error increases significantly. Thirdly, the interpolation step $\Delta\phi$ cannot be set too sparse, it should be no larger than 0.1°.

Assume that there are two uncorrelated narrowband signals which impinge on the array with the DOA of $\phi = 2\pi/9$ and $\phi = \pi/2$. The polarization of the signal is the same as the antenna element, and the

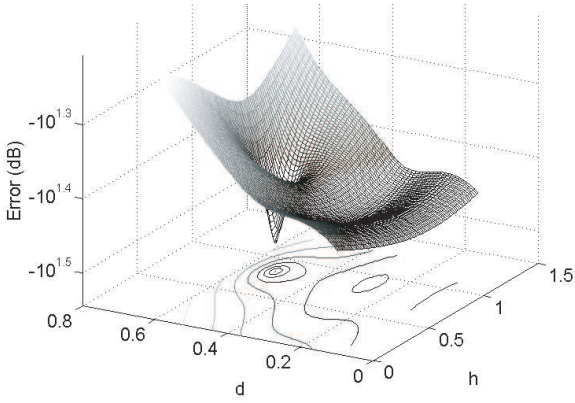

Figure 7. The relationship between error τ in Equation (10) and the virtual array's parameters d and h.

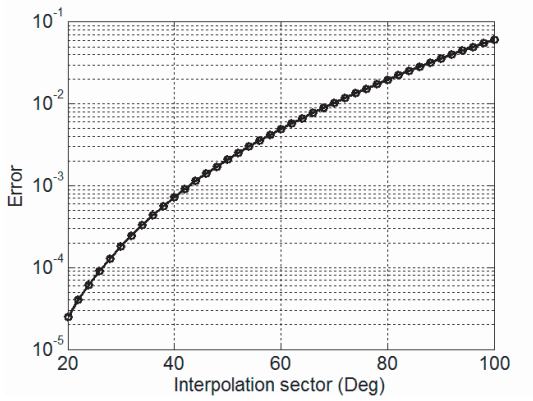

Figure 8. The relationship between error and the interpolation sector.

snapshots (sample points of the array) are 128. In this simulation, directional antenna elements with radiation pattern shown in Fig. 2 are used. The interpolation sector for each sub-array is set to $\pi/4$, and the interpolation step is 0.1°. 100 independent measurements are carried out. Sub-array divided MUSIC and 1-D Interpolated ESPRIT algorithms' performance are compared in Fig. 9(a) and Fig. 9(b).

For signal 1, when the signal's DOA $= 2\pi/9$, 8 elements can receive this signal (i.e., elements 1–6 and 15–16). Here we just need to compare the performance of sub-arrays 1–3. It is clear to see that the interpolated ESPRIT algorithm's performance in sub-array 1 is very similar to sub-array divided MUSIC algorithm because the signal is

close to its normal direction: $\phi = \pi/4$. The performance in sub-array 2 is a little bit weak compared to sub-array 1 due to the oblique incident angle. When SNR > 5, the RMS in these two sub-arrays are all within 1 degree. For sub-array 3, since elements 7–9 cannot receive the signal with DOA $= 2\pi/9$, the steering vector is incomplete; the algorithm in this sub-array is out of work, so the results are totally wrong. Because signal 1 is in sub-array 1's observation sector, we accept sub-array 1's estimation result and reject others.

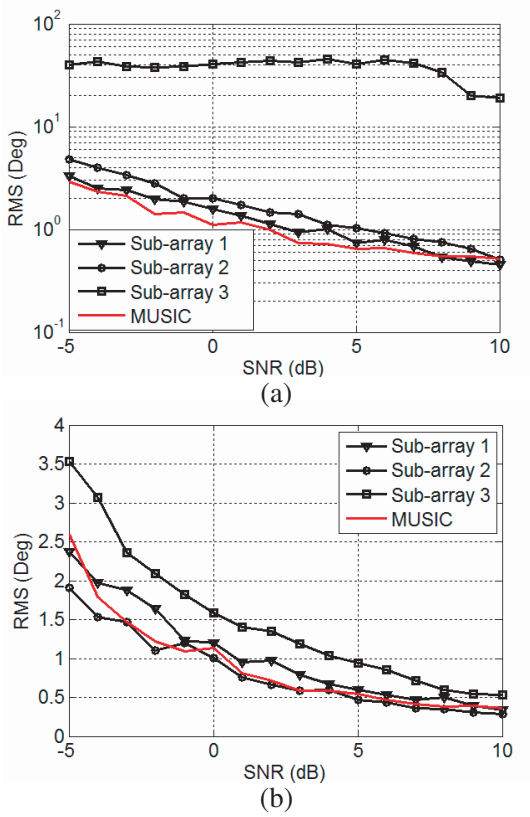

Figure 9. (a) The estimation RMS error versus SNR for 1-D case. DOA $= 2\pi/9$. The red solid line is sub-array divided MUSIC algorithm; other three black lines are interpolated ESPRIT algorithm of three sub-arrays. (color online). (b) The estimation RMS error versus SNR for 1-D case. DOA $= \pi/2$. The red solid line is sub-array divided MUSIC algorithm; other three black lines are interpolated ESPRIT algorithm of three sub-arrays.

Similarly, for signal 2 with DOA $= \pi/2$, 9 elements can receive this signal (element 1–9), so for sub-array 1–3, the steering vectors are all complete. Both sub-arrays 1 and 2 have the same performance as MUSIC algorithm. When SNR > 0, their errors are all smaller than 1 degree. Sub-array 3 has a relative weak performance because the radiation pattern is not totally symmetrical.

For 2-D case, in order to simplify the problem, we just use one sub-array to do the test, and for more sub-arrays, the method is similar for 1-D case. As shown in Fig. 5, 5 by 5 antenna elements are mounted on a metallic cylinder surface. The parameters of these antennas are the same as those in 1-D. The cylinder's radius is 1.28λ, and height is 4λ. Through interpolation technique, the conformal array

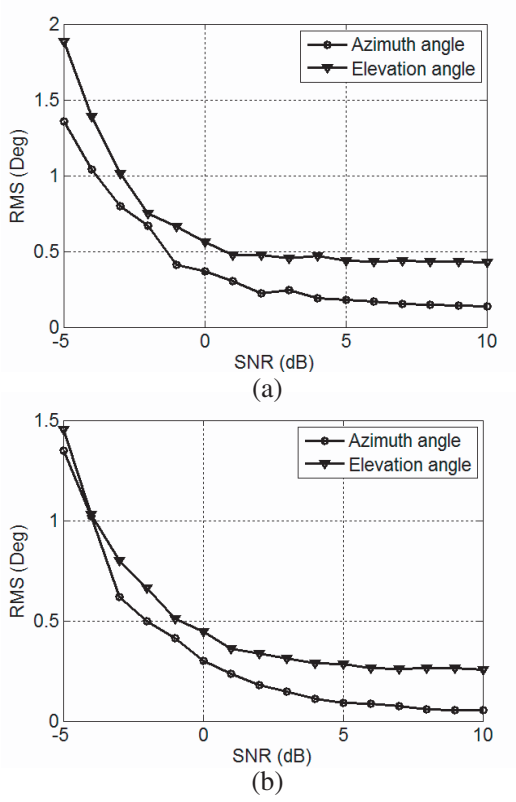

Figure 10. (a) The estimation RMS versus SNR for 2-D case, DOA $= (-5°, 110°)$. (b) The estimation RMS versus SNR for 2-D case, DOA $= (15°, 75°)$.

is transformed to uniform planar array with element distance of 0.5λ and omni-directional radiation pattern. The interpolation sector is chosen as: $\phi \in [-20^\circ, 20^\circ]$, $\theta \in [70^\circ, 110^\circ]$, and the interpolation step is 0.2°. It is worth to note in the 2-D case, each antenna element has a different radiation pattern due to different locations. Assume two signals with DOA $(\phi, \theta) = (-5^\circ, 110^\circ)$ and $(15^\circ, 75^\circ)$ incident on this array, other parameters are the same as 1-D example. 100 independent measurements are carried out. Figs. 10(a) and 10(b) show the interpolated 2-D DFT ESPRIT algorithm's estimation performance.

As shown in Figs. 10(a) and 10(b), two signals' DOAs are estimated accurately. When SNR $>$ 0 dB, the RMS are almost less than 0.5 degree. The difference of estimation performance for azimuth angles and elevation angles may be because the radiation patterns are not identical in these two directions. The large elevation incident angle of signal 1 makes the estimation performance in Fig. 10(a) worse than signal 2 in Fig. 10(b).

Table 1. Time consuming of two methods (100 simulations time).

	Interpolation	Estimation	Total
MUSIC (1-D)	—	4.5 s	4.5 s
Proposed method (1-D)	6.3 s	2.3 s	8.6 s
Proposed method (2-D)	334 s	5.2 s	339.2 s

The complexity of the spectral searching of the conventional MUSIC-based algorithms are too high for real-time applications. Here we compare the proposed method and the sub-array divided MUSIC algorithm's time consuming. The PC with Intel Xeon 2.66 GHz and 12 G ram are used for simulation. 100 experiments are carried out. In these tests, three sub-arrays (1–3) are used. The interpolation step is 0.1° for 1-D estimation and 0.2° for 2-D estimation. The results are shown in Table 1. From Table 1, we can see that for 1-D problem, the proposed ESPRIT-based method takes 6.3 s for interpolation and 2.3 s for estimation. The estimation time is about half of MUSIC-based method. For 2-D problem, it takes a long time for interpolation, about 334 s, but the estimation time is just 5.2 s, a little bit longer than 1-D problem. Though the time for 2-D problem of MUSIC-based method is not given here, we can imagine that 2-D space searching will take a much longer time than 1-D searching.

The method proposed above is a universal method and can be used not only for circular or cylindrical array but also for other array shapes. To verify its universal character, a parabola array shown in

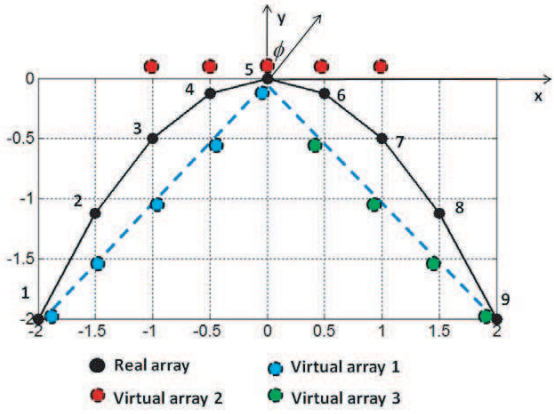

Figure 11. Parabola array for DOA estimation. 9 elements are divided into 3 sub-arrays.

Fig. 11 is used for testing. This parabola array has a mathematical expression of $y = -0.5x^2$. There are 9 elements distribute with equal x interval. Next, we divide the array into 3 sub-arrays, elements 1–5 as sub-array 1, elements 3–7 as sub-array 2, and elements 5–9 as sub-array 3. Then, by using interpolated technique, three sub-arrays are transformed to three uniform linear arrays (shown in Fig. 11). The searching region of the parabola array is also divided into three sectors: The searching sector of sub-array 1 is from $\phi = -\pi/3$ to $\phi = -\pi/9$, $\phi = -\pi/9$ to $\phi = \pi/9$ for sub-array2 and $\phi = \pi/9$ to $\phi = \pi/3$ for sub-array 3. The sub-arrays and sectors need not be identical. How to divide them is determined by how to get the smallest transform error in Equation (10).

Suppose there are two signals incident on the array with $\phi_1 = -\pi/4$ and $\phi_2 = \pi/12$, where ϕ is the angle with y-axis. To simplify the problem, suppose each element has an omni-directional pattern. The estimation results are shown in Fig. 12(a) and Fig. 12(b). It can be seen that two signals are estimated accurately. For signal 1 ($\phi_1 = -\pi/4$), sub-array 1 has a higher performance than sub-array 2 because the direction of signal 1 is at the normal direction of sub-array 1. The same result happens to signal 2 ($\phi_2 = \pi/12$), which direction is closer to the normal direction of sub-array 2, so sub-array 2 has a higher performance in this case.

Generally speaking, for a certain array, we can always divide it into several sub-arrays, and these sub-arrays need not be identical. They can be composed of different numbers of elements, different element

intervals, or different interpolations and searching sectors. The only limit is that each sub-array must have a "complete" steering vector (i.e., all elements of the sub-array can receive the signal that comes from corresponding sector). However, the estimation performance of each sub-array may be different, because when we do the virtual transform, the transform error (τ in Equation (10) may be different. Sometimes, for example, if the array with a small curvature radius, it may be difficult to find a virtual array to make the error in Equation (10) small enough. How to find the best virtual array is an optimization problem and will be studied in our future work.

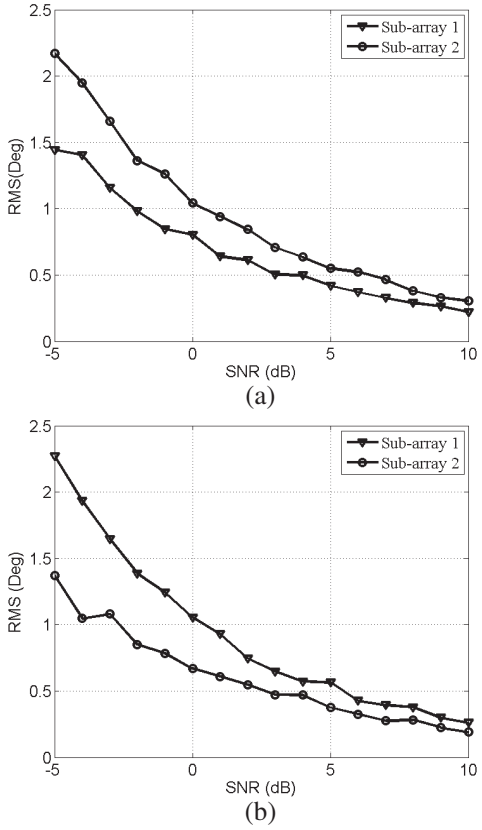

Figure 12. (a) The estimation RMS error versus SNR for parabola array. The incident DOA is $\phi_1 = -\pi/4$, sub-array 1 has a higher performance. (b) The estimation RMS error versus SNR for parabola array. The incident DOA is $\phi_2 = \pi/12$, sub-array 2 has a higher performance.

4. CONCLUSION

A new search-free DOA estimation method based on conformal array is proposed. In this method, there are three key techniques: Firstly, to avoid the "shadow effect" coming from the platform, the array is divided into several identical sub-arrays. Secondly, because ESPRIT-based algorithm cannot be used directly in these curved sub-arrays with directional antenna elements, an interpolation technique is used to transform these curved arrays to uniform linear array or uniform planar array with omni-directional elements. Thirdly, using 1-D LS-ESPRIT or 2-D DFT ESPRIT algorithm in these virtual arrays, signal's DOA can be found quickly and accurately. This method has a universal character and can be applied to any arbitrary conformal arrays. Numerical simulations confirm that this method has much faster speed with the same accuracy compared to other space searching based methods, such as MUSIC algorithm.

ACKNOWLEDGMENT

This work is supported by NASF (No. 10876007) and GADF (No. 9140A01020109DZ0202).

REFERENCES

1. Josefsson, L. and P. Persson, *Conformal Array Antenna Theory and Design*, IEEE Press Series on Electromagnetic Wave Theory, 2006.
2. Balanis, C. A., *Antenna Theory: Analysis and Design*, Wiley, New York, 2005.
3. Tuncer, E. and B. Friedlander, *Classical and Modern Direction of Arrival Estimation*, Elsevier, Burlington, MA, 2009.
4. Schmit, R. O., "Multiple emitter location and signal parameter estimation," *IEEE Trans. Antennas Propag.*, Vol. 34, No. 3, 276–280, Mar. 1986.
5. Roy, R. and T. Kailath, "ESPRIT-estimation of signal parameters via rotational invariance techniques," *IEEE Trans. Acoust., Speech, Signal Process.*, Vol. 37, No. 7, 984–995, Jul. 1989.
6. Peng, Y., Y. Feng, and Z. Nie, "DOA estimation using MUSIC algorithm on a cylindrical conformal antenna array," *IEEE Antennas and Propagation Symposium*, 5299–5302, 2007.
7. Mathews, C. P. and M. D. Zoltowski, "Eigenstructure techniques

for 2D angle estimation with uniform circular arrays," *IEEE Trans. Signal Processing*, Vol. 42, No. 9, 2395–2407, 1994.

8. Friedlander, B., "Direction finding with an interpolated array," *Proc., ICASSP*, 2951–2954, Albuquerque, NM, Apr. 1990.
9. Weiss, A. J. and M. Gavish, "Direction finding using ESPRIT with interpolated arrays," *IEEE Trans. Signal Processing*, Vol. 39, No. 6, 1473–1478, 1991.
10. Friedlander, B. and A. J. Weiss, "Direction finding for wide-band signals using an interpolated array," *IEEE Trans. Signal Processing*, Vol. 41, No. 4, 1618–1634, 1993.
11. Yuen, N. and B. Friedlander, "Asymptotic performance analysis of esprit, higher order esprit, and virtual ESPRIT algorithms," *IEEE Trans. Signal Processing*, Vol. 44, No. 10, 2537–2550, Oct. 1996.
12. Hwang, S. and T. K. Sarkar, "Direction of arrival (DOA) estimation using a transformation matrix through singular value decomposition," *IEEE Antennas and Propagation Symposium*, 130–133, 2005.
13. Rubsamen, M. and A. B. Gershman, "Root-MUSIC based direction of arrival estimation methods for arbitrary non-uniform arrays," *Proc., ICASSP*, 2317–2320, 2008.
14. Zoltowski, M. D., M. Haardt, and C. P. Mathews, "Closed form 2-D angle estimation with rectangular arrays in element space or beamspace via unitary ESPRIT," *IEEE Trans. Signal Processing*, Vol. 44, No. 2, 316–328, Feb. 1996.